Lahars Deposits Architecture and Volume in the C. Lengkong Valley at Semeru volcano, Indonesia

Christopher Gomez, Franck Lavigne, Danang Sri Hadmoko

Lahars Deposits Architecture and Volume

in the C. Lengkong Valley at Semeru volcano, Indonesia

Gomez C., Lavigne F., Hadmoko Sri D.

Gomez C.

Université Paris 7 – Denis Diderot,

Laboratoire de Géographie Physique CNRS UMR 8591,

1 Place Aristide Briand, 92190 Meudon, France

e-mail : christophergomez1101@yahoo.com / christopher.gomez@cnrs-bellevue.fr

Lavigne F.

Université Paris 1 – Sorbonne

Laboratoire de Géographie Physique CNRS UMR 8591,

1 Place Aristide Briand, 92190 Meudon, France

Hadmoko Sri D.

Université Paris 1 – Sorbonne & Univ. Gadjah Mada (Indonesia)

Laboratoire de Géographie Physique CNRS UMR 8591,

1 Place Aristide Briand, 92190 Meudon, France

Abstract

Lahars at Semeru volcano, Indonesia, are an ongoing phenomenon that rapidly transports large amount of clastic materials, threatening populations and infrastructures on and at the foot of the volcano. Focusing on lahars' deposits, this contribution has three main aims: (1) Understand the terrasses and valley bottom deposits architecture and their eventual correspondence with GPR (Ground Penetrating Radar) electromagnetic signals; (2) Calculate volumes of removable materials inside the valley; (3) explain the deposits irregular distribution in the valley.

In order to reach these goals, we worked on a 4.2 km stripe of the Curah Lengkong valley, 8 km S-SE from the summit in an area favorable to lahar deposits. We used a geomorphological approach, completed with an extensive GPR campaign over the terrasses and deposits at the bottom of the valley. We also analyzed a series of aerial photographs that we converted into GIS in order calculate lahars' terrasses volumes, and in order to understand their spatial distribution.

Results highlight that the terrasses' architecture is typically divided into horizontal units, with "progradation like" lateral variations, whereas deposits at the bottom of the valley are not presenting any clear architecture. The calculated volume of lahar deposits is 0.51 million cubic meter for the 4,2 km channel

section we studied. This overall volume is divided between 210,200 m^3 for the terrasses and 301,000 m^3 for the bottom of the valley. These deposits are unevenly spread through the valley since they are mostly concentrated in the upstream half of the valley, with 25% of the material located within the first 500 meters. We could identify to concentration areas that are due to (1) a natural topographic jump and (2) the presence of a SABO dam that blocks the sediments. Therefore, this study emphasizes the role of local topography on deposits, and the importance of the “invisible” materials located at the bottom of the valley.

1. Introduction

Mt Semeru is an active volcano and the highest mountain in Java (3676 m a.s.l.). Its densely populated - 400-900 inhab./km^2 - lower flanks and ring plain are subject to lahar-related disasters. Those areas carry a lahar death toll overshooting a thousand people for the 20^{th} century alone.

The Semeru eruptive activity is characterized by continuous vulcanian-strombolian eruptions. From 1967 the volcano is producing short-lived eruption columns every 15 minutes in average. This activity is increasing every 5 to 15 years with higher eruption columns and ballistic bombs that can reach 8 km distance and ashfall that can travel downwind as far as 30

km. During these periods of increased activity small glowing avalanches are also occurring on the upper flanks. Collapses of summit domes, growing periodically in the crater open toward the southeast, generate block-and-ash flows and scoria flows, which enter the SE and east drainages as far as 5 to 11.5 km from the vent. In addition, lava flows occurred at fissures on the cone flanks at least twice during the past century (Fig.1).

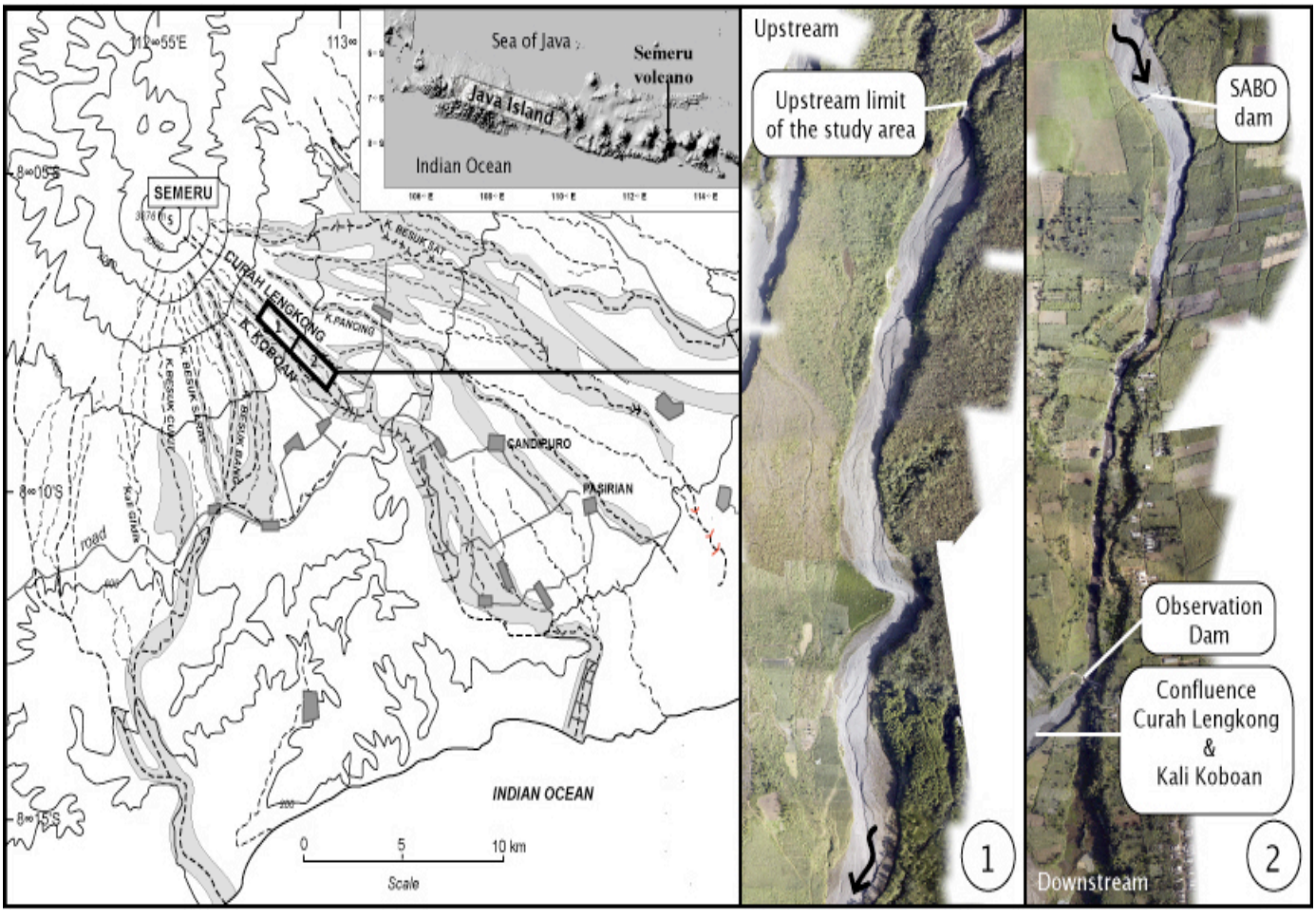

Fig. 1: Study area's location on Semeru volcano, East Java, Indonesia. The map shows the lahars inundation zone for the 20th century largest events (Adapted from Thouret et al., 2007). The study area is limited upstream by a natural fall created by a lava deposit, and downstream the confluence between the Kali Koboan and the Curah Lengkong. At the observation dam, a French – Japanese collaboration set up a video camera system, and recently large sediments' traps.

According to Lavigne and Suwa (2004), lahars at Semeru can be (1) syn-eruptive lahars, occasionally generated when a drainage system is choked by a pyroclastic flow, (2) secondary and post-eruptive lahars – majority -, i.e. triggered by rainfall on loose pyroclastic material. Yet some non-eruptive lahars – i.e., unrelated to eruptions – may occur through processes common to volcanic terrains, such as landslides or flank collapse (e.g., in 1909 and 1981).

Tens of small-scale lahars ($Q<400$ m^3/s) are commonly triggered by high intensity monsoon storms during the rainy season from October to April (Lavigne and Suwa, 2004). Three factors favour the generation of the most serious lahar hazard at Mt Semeru: (1) the volume of primary pyroclastic debris shed around the summit is estimated at 4×10^4 m^3/yr each year (Siswowidjojo et al., 1994); (2) a dense drainage network of at least ten high-gradient rivers convey sediment on steep slopes of the cone towards the east and SE ring plain over a distance of 15-35 km, and; (3) annual rainfall amounts up to 3000-3500 mm. On 23-24 September 1998, a 500 mm rainfall during 48 hours on the SE flank triggered a lahar, which lasted 17 hours with a discharge of 300 m^3/s.

Sedimentologic and hydrologic parameters of rain-induced lahars have been measured at 9.5 km from the summit in the Curah Lengkong (825 m asl.), a tributary to Koboan River. In

2000, each of eight largest lahars transported a volume of 4-5.7 x 10^5 m^3 (Lavigne et Suwa, 2004). Each event emplaces as much as 4 to 6 beds of hyperconcentrated-flow and matrix-supported debris-flow deposits totalling 0.8 to 3 m in thickness. Albeit non cohesive, these debris-flow deposits contain a large amount of sand ash supplied by the scoria- and ash-rich pyroclastic flows. Velocity was in the range of 1.5-7.5 m/s; discharge in the range of 85-280 m3/s varies widely in debris flows.

In the Lengkong River catchment (28.5 km^2), erosion caused an annual sediment discharge of as much as 2.7 x 10^5 m^3/km^2 in 2000 (Lavigne, 2004). The specific denudation rate is about 4.4 x 10^5 $t/km^2/yr$. These high sediment yield and denudation rates compare well with other values reported on active composite cones in humid environment (Major et al., 2000). In contrast to these cones, however, sediment yield at Semeru does not decline drastically within the first post-eruption year. This is due to the steady supply of clasts shed in the summit area, which can be remobilised by runoff any time during the rainy season and even during the 'dry' season.

Our investigation was carried out over a 4,2 km length stripe in the Curah Lengkong valley that extend from 3.8 to 8 km S-SE from the summit of the Semeru volcano. This portion of the valley is limited upstream by a wall built in a lava flow deposit and downstream we limited our investigations at the confluence

with the Curah Koboan, just down the location we set up the video-camera system that allowed us to conduct previously mentioned studies on lahars.

This contribution addresses two main issues related to the Mt Semeru lahars deposits: (1) a description of their characteristics and architecture (2) the calculation of removable volumes for the 4,2 km study area.

2. Methodology

For this study we compounded: (1) a quantitative and qualitative geomorphological investigation on lahars' deposits; (2) a geophysical method – Ground Penetrating Radar (GPR); and (3) an alternative method to stereophotogrametry based on cast shadows from aerial photographs that ended up into a GIS.

2.1 Field investigation: geomorphology and GPR

At first, we measured the morphometry of the valley bottom and the lahars' banks deposits using a laser rangefinder and a GPS. We completed these measures with (1) samples from lahars' banks for grain-size analysis, (2) and some qualitative observations on material characteristics, on banks' facies and layering, mainly for GPR calibration.

In a second time we organized a GPR campaign divided into (1) a series of longitudinal transects at the bottom of the river (500 Mhz); (2) a few transects on selected lahars' banks (500Mhz & 800Mhz). The GPR used for this study is a standard commercial RAMAC. The GPR produces electromagnetic waves that are controlled by the dielectric permittivity, electric conductivity and magnetic permeability. Thus causes of signal variations are often difficult to clearly identify. Because of these difficulties, we calibrated the radar signal patterns against stratigraphic exposures and material characteristics as it is commonly done (e.g. Lowe, 1985; Rust and Russell, 2000; Gomez-Ortiz et al., 2006). Once the signal was calibrated against outcrops we extended GPR investigations on banks and on the Lengkong River bed. After collection, we treated the data with the software Reflex®, in order to improve the visuals, convert velocities into depth, and introduce topographical data.

2.2 Aerial photographs analysis

For this study, we did not have aerial photographs that allowed us to perform stereophotogrametry; therefore we elaborated a simple alternative method based on cast shadows (Fig. 2). The bottom of the Lengkong valley is horizontal or close to horizontal, and lahars banks deposits have subvertical edges. Thanks to these particularities we measured the angle between

the floor and the sun elevation in order to establish a relation between cast shadows of lahars banks and their height. Thus we measured the cast shadows on the aerial photographs parallel to the azymuth orientation – 64.25 degree from North – and multiplied it by the tangent of the sun elevation. The result of this calculus gives the banks' height. Photos were taken between 9:32AM and 9:35AM, therefore we considered the sun position as fix for the all set of photographs.

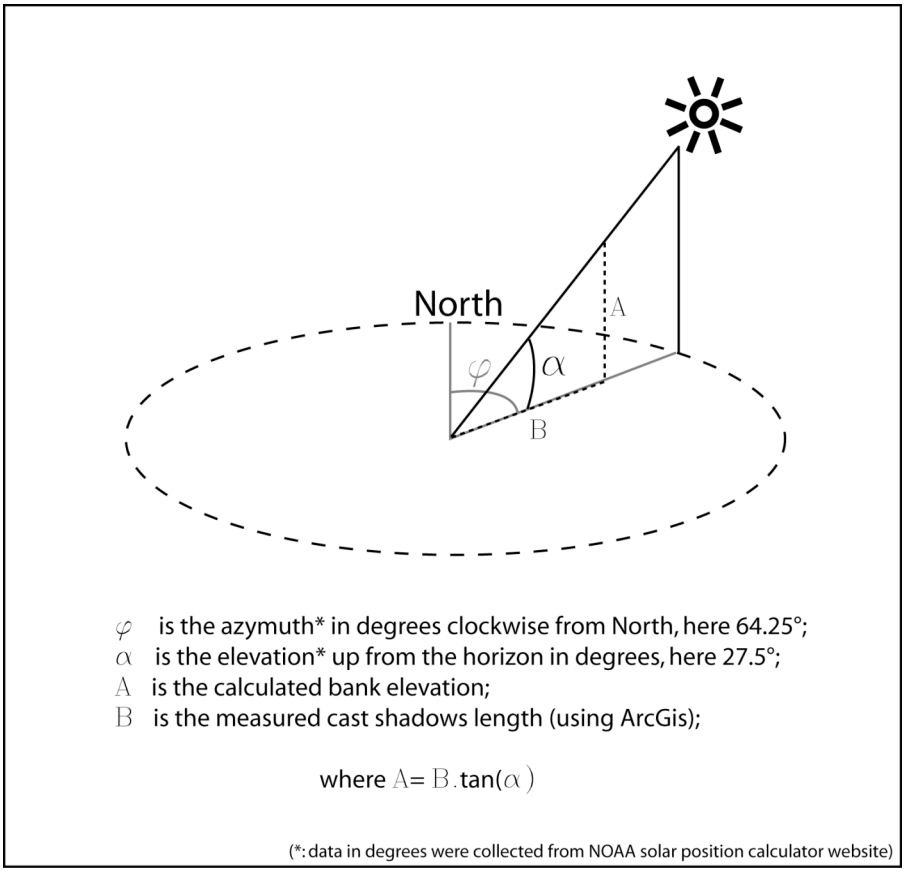

Fig. 2: measure of the sun position in the sky, and the cast shadows. For lahar deposit and valley bottom, this measure offers a simple and economic way to replace ortho-photographs, if they are not available.

The second step dealt with computing the data into a GIS in order to retrieve the banks surface, and therefore calculate their volumes, and analyze their distribution in the valley. Due to the images limitations, we mainly measured banks with a height ranging from 2m to 8.8 m. Then, we combined them with surfaces calculated from the aerial photographs.

3. Results

For this study we worked on all deposits that were within the Curah Lengkong valley, however we emphasized our banks architecture's investigation on the deposits of the largest lahar that occurred on April 12th 2006, because (1) it left the largest amount of deposits; (2) we studied its flow behavior in a companion paper to be published (Cf. chapter 6).

3.1 Banks and valley bottom architecture

Terrasses deposits of the 12th April 2006 lahar are mainly composed of coarse clasts with almost no silt or clay, which is typical of non-cohesive lahars. Deposits are organized in horizontal layers, separated by thin layers of well-sorted silty to sandy material. These deposits can have different origin, as we learned in chapter 6. They can either be sole layers, deposited at the base of the flow, or deposits from hyperconcentrated-

flows or deposits linked to flow avulsion. At its thickest location – thickness = 2.40 m - 3000 from the upstream limit of the study area - the deposit has an architecture that comprises 4 horizontal units. They are respectively 56 cm 64 cm, 35 cm and 106 cm from top to bottom (Fig. 3).

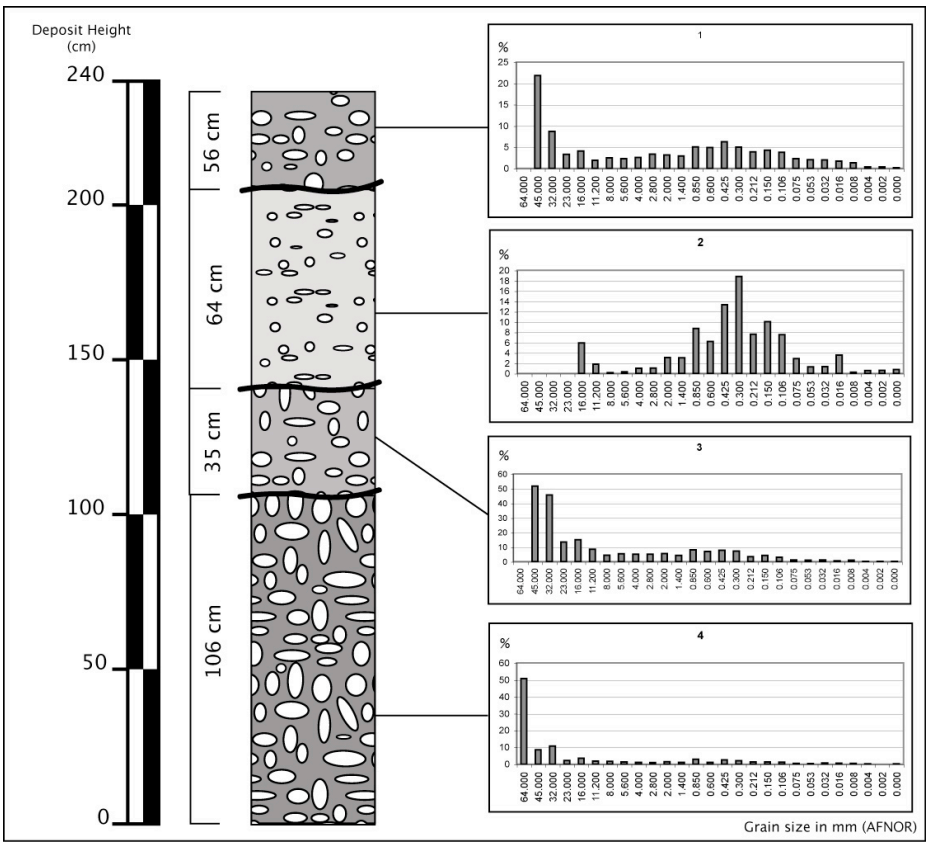

Fig. 3: The 12th April lahar deposit stratigraphy and grain size at its thickest location. The unit 1 (upper unit) has a bimodal grain-size distribution, with numerous blocks inside a sandy matrix. The unit has only one mode, with a majority of sandy materials. The unit 3 has been conserved as it was after laboratory analysis. However this unit can't be considered for interpretation, since there is an error in the measurements. The total of all the fractions is superior to 100%. Based on the field visuals though, the graphic should have the same global trend, with a majority of cobbles in a sandy matrix. In the end, unit 4 is dominated by elements which size is superior to 32 mm.

The grain-size of the first unit is a bimodal statistic distribution, which is characteristic of debris-flows phases, with a large proportion of boulders inside a sandy matrix. This unit is showing a slight reverse gradient in grain-size. The second unit, located just below has one mode that emphasizes the presence of coarse sands. The distribution is close to a bell-shape, characteristic of hyperconcentrated flow phases. The third unit is characterized by a large number of cobbles in a sandy matrix – as we had visual confirmation on the field -, however, measurements' errors at the laboratory in Indonesia want us not to consider this data for further interpretation. In the end, the unit 4 is characterized by a large presence of boulders with a coarse sand matrix. Larger boulders were also observed on the field, even though it was impossible to bring them back to the laboratory. This unit is characteristic of the front deposit, with the boulders abandoned on the side of the front (Lavigne and Suwa, 2004).

Downstream, this deposit's depth and number of unit diminish. It has only 3 units at the foot of the dam that mark the downstream limit of the study area. At this location, the deposit's architecture is not horizontal, but presents a downstream skewed shape. The units are composed of coarse sands and pebbles, separated by thin horizons of silty material.

Against these direct observations, we compared the GPR radargram, drawn from this location (Fig. 4).

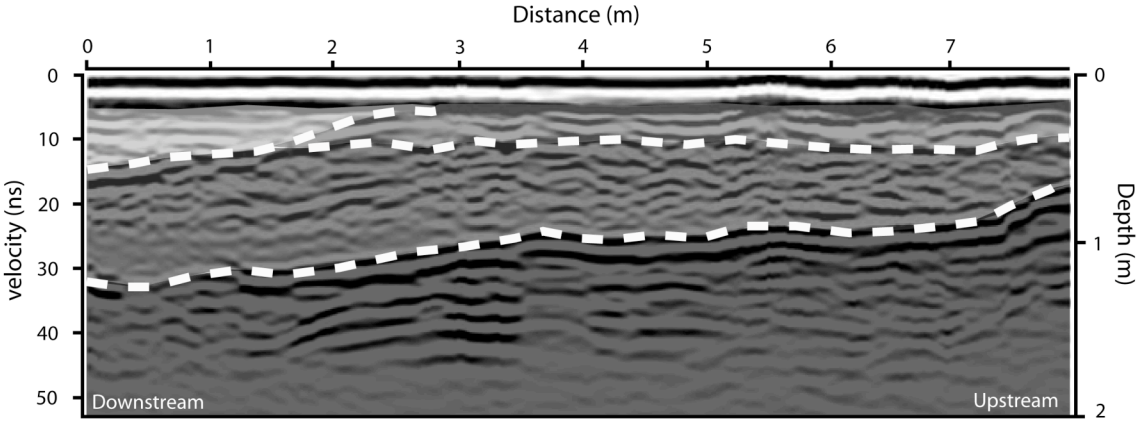

Fig. 4: The three units of the 12th April lahar, down the observation dam. On this modified radargram, we distinguished the units we directly observed on the field with different tints of grey, and a dot-line separator. The actual separation between these units is characterized on the field by thin horizons of silty material, whereas a coarse sands matrix mainly composes the main units. On the radargram, we can see, within these units, the presence of a more complex architecture, with other contact layers, and the presence of punctual elements that create hyperbolas.

It obviously appears that grain-size variations influenced the electromagnetic signal. Indeed thin layers of silty material gave a distinctive reflective horizon on the radargram, which rendered a net distinction between the three units of coarse elements. It also clearly rendered the deposit's architecture with its downstream skewed shape. The radargram is not bringing any new information for these outcrops that we could not get visually, but it is important to note that we can retrieve the deposits architecture, based on the grain-size variations. Hence,

it is possible to extend radargram away from outcrops, and work on the lateral architecture of lahars' terrasse, that do not offer visual confirmation.

At the confluence of Curah Lengkong Valley and the Curah Koboan Valley, we studied the architecture of terrasses from both valleys, and evidenced the way they overlap (Fig. 5). Thanks to the radargram, we could retrieve 9 different units (units A to I) inside the deposit, although we don't have a clear image of the first centimeters, because of the surface echo (J). All units are characterized by numerous hyperbolas that are characteristics of the presence of numerous blocks (the radargram does not offer any precision on their size). Each of these units are separated by strong reflective horizons, like it was the case for the radargram corroborated with the bank (presented above).

The limits are not all clear though. For the two units "A" and "D", it is difficult to define a precise limit. Nevertheless, we can still evaluate the order of deposition of the different Units. Hence, the two first units that deposited are "D", and "E" followed by "A", because this last one is slightly covering the edge of "E". Then "B" deposited. The other units don't have enough contact area to know the exact deposit order. Indeed unit "C" deposited after "B" and "E", and before "I" and "H", but there are no other evidences we can use. In the end units "I" and "H" deposited.

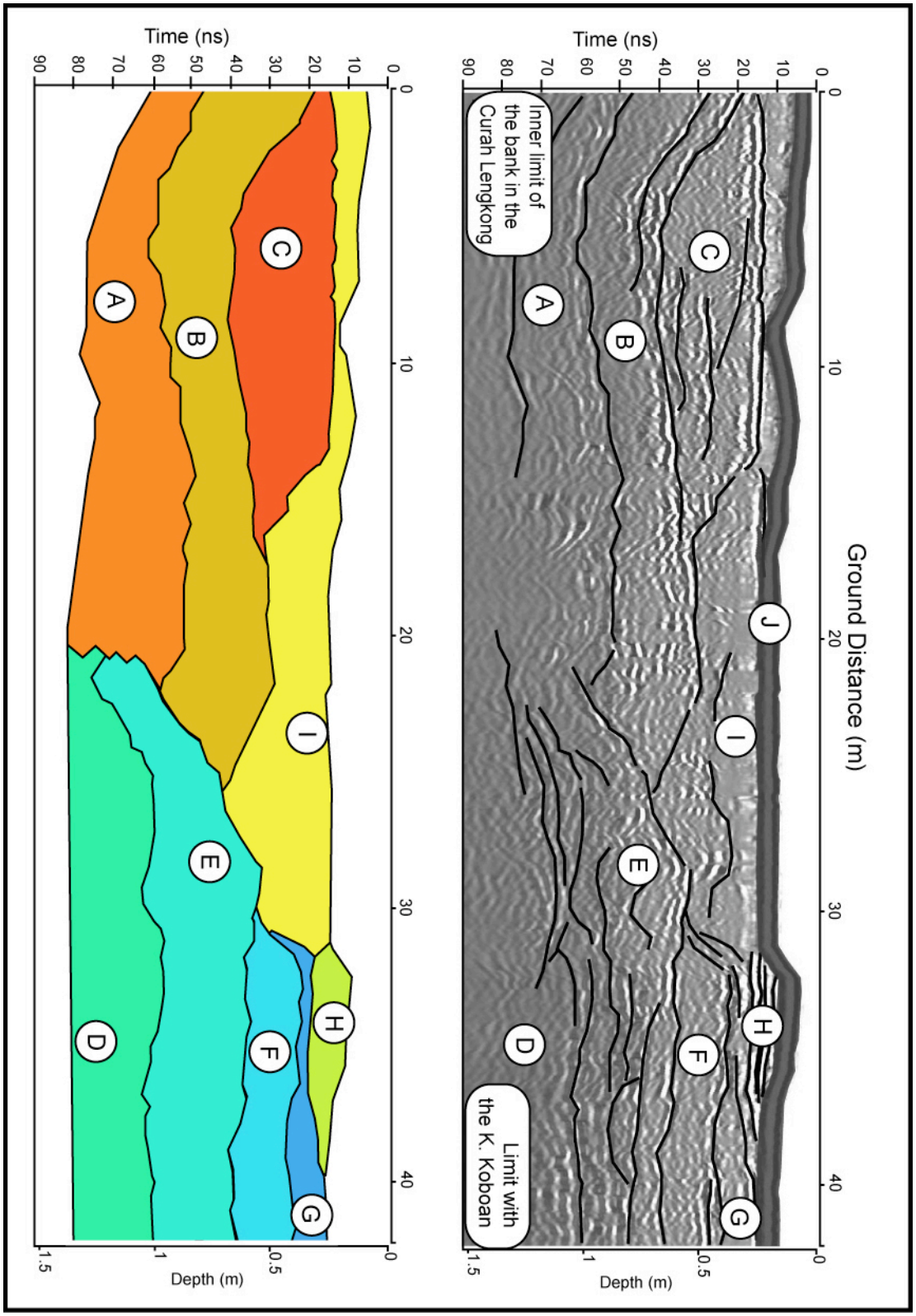

Fig. 5: GPR transect on the Curah Lengkong's right bank at the confluence with the Curah Koboan. The letters A to I indicate different units inside the bank deposit. Strong reflective horizons differentiate the units. The schema in color below shows these different units. This is a non-exhaustive method, and the numerous smaller units certainly remain unveiled.

Based on direct visual observations we could confirm units “I” and “H” as lahar deposits, “H” being almost totally eroded. Unit “G” is a leak from a pyroclastic-flow deposit that come from the Kali Koboan. Other units could not be visually confirmed, but there are no pyroclastic-flow recorded in the Curah Lengkong until this distance, therefore units “A”,”B” and “C” are certainly lahars deposits as well. They are either different units from a single lahar, or more probably different lahars deposits.

Deposits at the bottom of the valley are more composite than those of the terrasses, because they involve a wider variety of materials: lahar deposits (wet or dry), lava flow deposits, and undetermined mixed interfaces. Based on these differences we retrieved an imagery of the valley’s subsurface in the lower part of the valley - between lines 3500 m and 4000 m (Fig. 6). The slowest velocities – 0.037 m/μs - characterize the lower part of the radargram. It corresponds to the thickest unit we detected and it can reach locally 3 m depth on the radargram - although it might be thicker, being out of range. This unit is locally reaching the surface, and by analogy we could classify it as an andesitic lava deposit.

On top of this unit extends a thick group of different units that we could not differentiate from any apparent architecture or horizon. This material corresponds to loose lahar deposits.

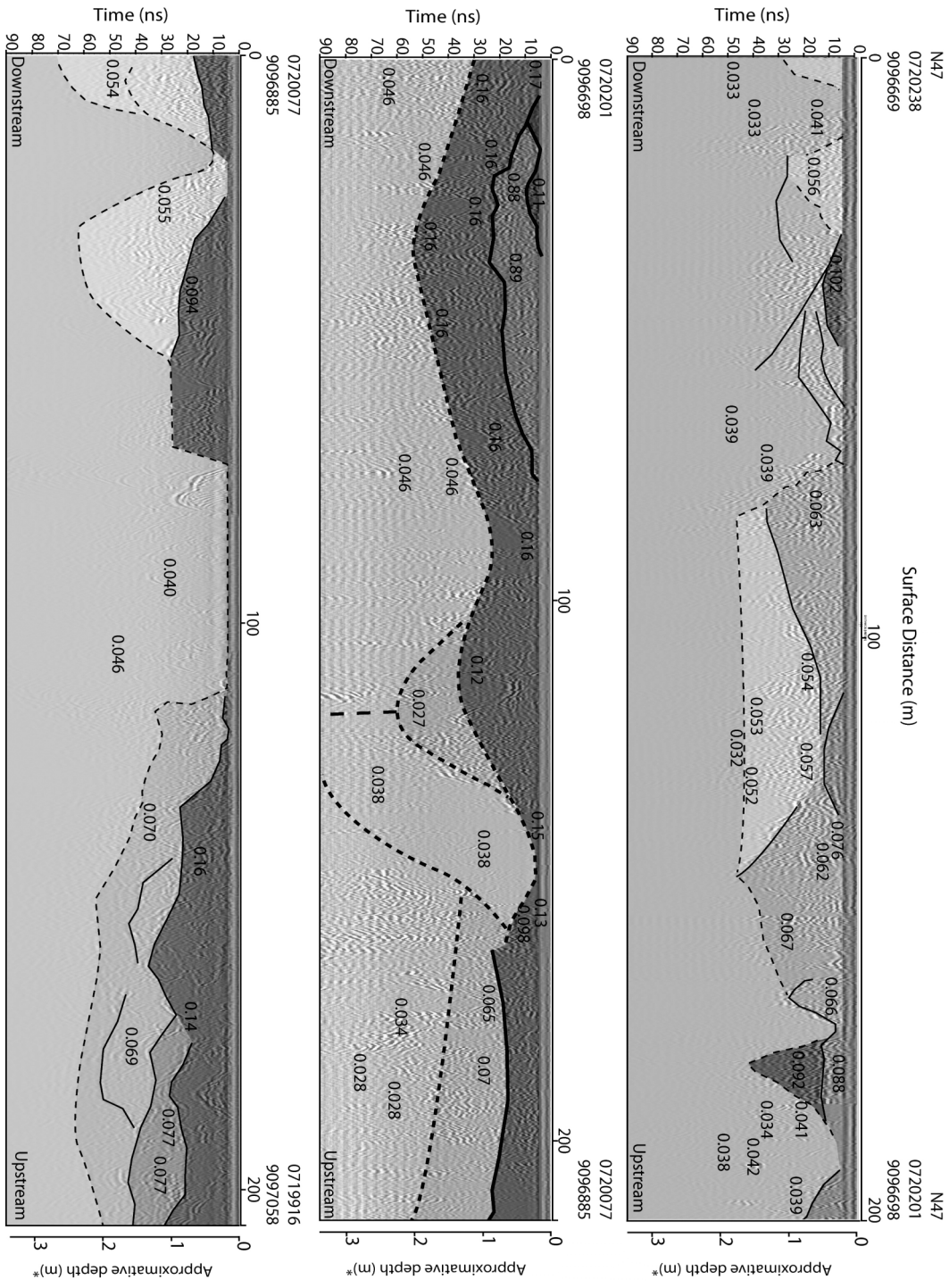

Fig. 6: Longitudinal radargram at the bottom of the Curah Lengkong valley, on a bit more than 600 m. The units are graphically discriminated with the help of different grey tints, depending on the GPR signal velocity. The lower part is characterizes by slow velocities. We identified this unit as a lava deposit by analogy with visuals we had on the surface of the deposit. The upper units seem to be all lahar deposits with various proportions of water content, as far as the visual observation can account for the one located below.

Nevertheless, we recorded important variations in the electromagnetic waves velocities - between 0.056 m/μs and 0.16 m/μs. Based on surface observations we can concur that those variations are due to change in water content. Faster velocities characterize wet surfaces and volumes, whereas dry surfaces and volumes tend to generate lower velocities.

Hence, lahar deposit architectures are very distinct, whether we study terrasses or the bottom of the valley. Respectively, the first one is characterized by horizontal or sub-horizontal layers that laterally prograded from the outer limits towards the center of the valley, whereas the second one do not display any clear architecture, and appears massive and unsorted with blocks distributed at random.

3.2 Distribution and volume of removable material

In order to estimate volumes of removable materials in the Curah Lengkong valley we took in consideration two stocks of materials (1) lahars terrasses, and (2) removable materials at the bottom of the valley.

(1) The volume of terrasses is ranging between 189 m^3 and 34,666 m^3 (Tab. 1), with an overall volume of 210,212 m^3 for all terrasses along the 4.2 km length of the study area. This corresponds to more than 50 m^3 per meter of channel length –

or 55 m^3/m of channel length if you consider the length to be 3.8 km. The terrasses' distribution is uneven along the valley and deposits are mainly concentrated within the two first kilometers upstream (Fig. 7).

Number	**Area** (m^2)	**Cast shadow**	**Terrasse thickness** (m)	**Terrasse Volume** (m^3)
1	392	5	2.4	941
2	4124	4	2	8248
3	1223	5	2.4	2935
4	8305	8	3.8	31559
5	2508	4	1.9	4765
6	1139	4	1.9	2164
7	6878	8	3.8	26136
8	2613	5	2.4	6271
9	1458	5	2.4	3499
10	1523	3	1.4	2132
11	6174	5	2.4	14818
12	739	5	2.4	1774
13	3259	9	4.1	13362
14	261	3	1.4	365
15	716	8	3.8	2721
16	3988	3	1.4	5583
17	5420	3	1.4	7588
18	1317	3	1.4	1844
19	14444	5	2.4	34666
20	5071	6	2.9	14706
21	1926	4	2	3852
22	2075	4	2	4150
23	5515	4	2	11030
24	135	3	1.4	189
25	113	3	1.4	158
26	680	4	2	1360
27	655	3	1.4	917
28	839	3	1.4	1175
29	371	3	1.4	519
30	561	3	1.4	785

Tab. 1: Thickness and volume of the main terrasse deposits in the Curah Lengkong, with bank 1 located the most upstream and the last one, terrasse 30, located the most downstream.

Indeed 25% of the material is concentrated within the first 500m, 50% within the first 1500m; and 92% at more than 2000 m. The repartition is also unbalanced between the left and the right side of the valley, where 23 of the 30 measured banks lie on the left side of the valley, with more than 80% of the deposits volume for the left banks. Terrasses concentration is driven by two main factors at the studied area: (1) the presence of a fall, like the dam downstream the study area, or the lava subvertical limit, upstream, which reduce the flow energy; (2) bends of large amplitude in the channel, which dissipate the energy of the flow and favor sediment deposition.

(2) The volume of removable materials at the bottom of the valley was measured from two parameters: the valley's surface (208,039 m^2) and the depth of removable materials (mean = 1.45 m). We considered that lahars, pyroclastic deposits, and unwelded tephras, deposits were removable. On the opposite lava was not incorporated, because it is resistant to lahar erosion. The volume of material available at the bottom of the valley for the 4.2 km studies is estimated to 301,600 m^3 (for an error margin estimated to be about 20% maximum, the volume is ranging between 241,000 m^3 and 362,000 m^3). Therefore the overall volume of materials potentially removable by lahars is 511870 m^3 for the studied section of the valley (or between 451,210 m^3 and 572,200 m^3 if you include the 20% error

margin). This represents 42% of the removable material is comprised in the terrasses and 58% at the bottom of the valley.

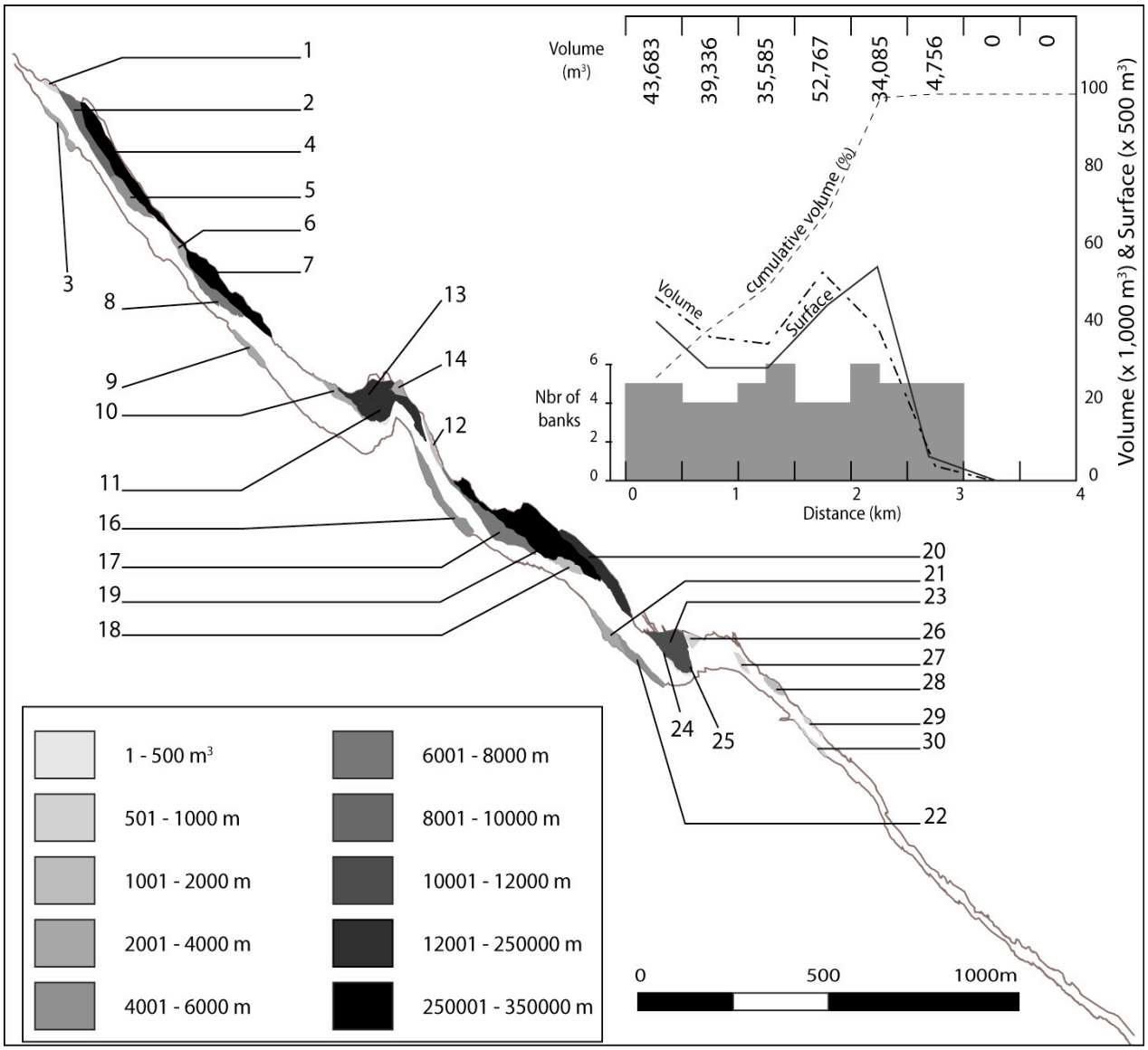

Fig. 7: Distribution map and chart of the lahar terrasses' deposits by volume in the Curah Lengkong valley. The majority of the deposits are concentrated in the upstream half of the valley, with two concentration zone between 0 m to 500 m and between 1800 m to 2500 m. These map observations are confirmed by the graphic, with 43,683 m^3 of terrasses deposits in the first 250 m and a second peak between 1500 m and 2000 m with 52,765 m^3. We can notice that the volumes' curve does not perfectly fit the surface curve, so that deposits' thickness plays an important role in the volume determination.

4. Discussion

This contribution brings six principal results: (1) The terrasses' deposits architecture due to grain-size variations can be retrieved with GPR; (2) The deposits' architecture varies longitudinally and transversally; (3) Terrasses' deposits present a clear architecture, whereas the bottom of the valley seem to have none; (4) The removable materials contribute both from the bottom of the valley and the terrases with unequal proportions. (5) The terrasses' deposits are unequally distributed along the valley, depending on the morphology of the valley.

The architecture of lahars' bank deposits can be successfully studied with GPR, at least when the deposits are not too oxidized nor with an important fraction of clays that stop the radar signal. The ability of the GPR signal to vary with grain-size is well known and this characteristic is widely used in earth sciences on other deposits, e.g. river basins (e.g. Sridhar et Patidar, 2005), etc. In volcanic areas though, GPR is often employed to characterize materials with a direct visual or combined with other geophysical techniques (e.g. Gomez-Ortiz et al., 2007), and it seldom separate from visual confirmation, since the results induced a part of interpretation then. However, recent studies are beginning to be interested in internal structures, extending away from direct visuals: e.g. for welded

zones in pyroclastic-flows deposits (Rust and Russel, 2000); the stratigraphy of hydrovolcanic fields (Cagnoli and Russel, 2000); internal structure of block-and-ash flow deposits (Gomez et al., 2008).

Understanding the architecture of the deposits, both in transversal and longitudinal orientations are essentials, especially for lahar deposits. Indeed, it brings a serious limitation to deposits analysis traditionally carried out from outcrops alone. Indeed the transversal variations in the deposit architecture, and notably the presence of lenses (Fig. 5) have two direct consequences: (1) an observation or measure made from a lahar bank outcrop can't be extended laterally, and it is not always representative of the deposit; (2) this same observation or measure from an outcrop is also not characteristic of the flow. Therefore, it is impossible to reconstruct the strict phases of a lahar from an outcrop alone, or even a series of outcrops.

Thus, the combination of radargrams with visual observations and measures can be of great help to understand the all lahar deposit architecture and deposition process. Cagnoli and Ulrych (2001) also cleverly brought this aspect for base surge deposits, the internal architecture of the deposit giving information on the flow direction, and therefore its origin, when this one is unknown.

The volume of removable materials including both banks' deposits and those at the bottom at the valley are of major importance, since it is prime results, but this data wants to be carefully interpreted since it has some limitations. Firstly we are just estimating the available stock of material. Indeed lahars erode unevenly the banks or the bottom of the valley, depending on the lahar size and its sediment concentration. The videos of the largest recorded lahar's front at Semeru volcano- shot by F. Lavigne in the C. Lengkong - is showing the lahars banks being instantly eroded by the large boulders (Lavigne et al., 2003), whereas videos of more modest lahars are showing banks that perfectly resists the erosive power of the flow (in a companion paper to be published). Moreover, if the debris flow phases can erodes the banks, hyperconcentrated phases tend to preferentially erode the bottom of the channel. Secondly, an other limits of these volume measures is to be related to how far they account for the all valley. Indeed the overall setting of our study area is at a slope break between the steeper slope upstream and the volcano foot with gentler slopes. Thus this location may be a favorable area for deposits compared to upper slopes. However, the presence of lava at the bottom of the valley in the study area may artificially reduce the amount of removable materials. Therefore, it seems difficult to extend these results to other part of the valley, and deduct overall removable materials in the valley.

In the end, the banks are unevenly distributed along the valley (Fig. 7), where most of the deposits are located in the upstream half of the valley, with two concentration zones. This uneven distribution is certainly driven by two elements: (1) the first concentration zone upstream is located just down a natural fall, where the lahars loose an important amount of energy, hence, the events tend to depose a large volume of material. (2) The second concentration zone is located just above a SABO dam that retains a large amount of lahars deposits, and artificially enhances the deposits volume. The presence of this SABO dam also explains the reason why there are only a few banks deposits in the downstream part of the valley, a large amount of sediments being stopped upstream the dam.

5. Conclusion

Despites a few limitations we expressed in the discussion, volumes of removable materials and the deposits' distribution expressed here are important for hazards estimation and engineering works like SABO dams constructions. It also gives us a glance at the various sedimentation problems linked to these constructions. In the end, the GPR also brings into light the limitations of traditional geological or geographical methods based on outcrops.

Acknowledgments: This work was supported by the Laboratoire de Géographie Physique, UMR 8591-CNRS (France), and funded by the INSU-CNRS through the ACI research program ‘Aléas et changements globaux’ (Hazards and Global Changes). We thank the two undergraduate students who accompanied us in the field: Marion Giffo and Cedric, the Semeru Volcano Observatory of The Geological Institute of Indonesia in Gunung Sawur, Mr Dodi and Darmono of the Mt. Semeru Project in Lumajang, and the Curah Lengkong village inhabitants for field assistance.